

A SUB-SATURN MASS PLANET ORBITING HD 3651¹

DEBRA A. FISCHER,² R. PAUL BUTLER,³ GEOFFREY W. MARCY,² STEVEN S. VOGT,⁴ AND GREGORY W. HENRY⁵

Received 2003 January 5; accepted 2003 February 25

ABSTRACT

We report precise Doppler velocities of HD 3651 obtained at Lick and Keck Observatories. The velocities reveal evidence of a planetary companion with an orbital period of 62.23 ± 0.03 days, an eccentricity of 0.63 ± 0.04 , and a velocity semi-amplitude of 15.9 ± 1.7 m s⁻¹. With an assumed mass of $0.79 M_{\odot}$ for this K0 V star, we derive $M \sin i = 0.20 M_J$ and a semimajor axis of 0.284 AU. The star is chromospherically inactive, with $\log R'_{\text{HK}} = -5.01$, and 10 years of observations at Fairborn Observatory show it to be photometrically stable to better than 0.001 mag. In particular, there is no photometric variability on the 62.23 day radial velocity period to a limit of 0.0002 mag, supporting the planetary interpretation of the radial velocity variability. Photometric transits of the planetary companion across the star are ruled out with a probability of 87%.

Subject headings: planetary systems — stars: individual (HD 3651, HR 166)

On-line material: machine-readable table

1. INTRODUCTION

More than 100 extrasolar planets⁶ have been discovered orbiting solar-type stars (see references in Butler et al. 2002) using high-precision Doppler observations to measure the reflex radial velocity of the host star. Most of these planets have $M \sin i$ comparable to or greater than Jupiter and induce stellar velocity amplitudes greater than 30 m s⁻¹. However, as Doppler precision increases, lower mass planets are being discovered. There are now five planet candidates with $M \sin i$ less than $0.3 M_J$, i.e., less than Saturn's mass: HD 16141 and HD 46375 (Marcy, Butler, & Vogt 2000), HD 16874 (Pepe et al. 2002), HD 76700 (Tinney et al. 2003), and HD 49674 (Butler et al. 2003). All of these except HD 16141 have orbital periods of less than 7 days and reside in nearly circular orbits. HD 16141 has an orbital period of 75 days with a modest eccentricity of 0.18. Here we report the detection of an additional sub-Saturn mass planet in an eccentric orbit with an orbital period of 62.2 days.

2. PROPERTIES OF HD 3651

HD 3651 (HR 166, HIP 3093) is a $V = 5.88$, $B - V = 0.85$, K0 V star. The *Hipparcos* parallax (ESA 1997) of 90.03 mas implies a distance of 11.1 pc and an absolute visual magnitude of $M_V = 5.65$. Our spectral synthesis model-

ing yields $T_{\text{eff}} = 5210 \pm 30$ K, $[\text{Fe}/\text{H}] = 0.05 \pm 0.05$, and $v \sin i = 1.7 \pm 0.5$ km s⁻¹. Based on the mass calibration tabulated in Allen's *Astrophysical Quantities* (Drilling & Landolt 2000), we adopt a mass of $0.79 M_{\odot}$ for this solar metallicity star.

To check for velocity variations, or “jitter,” that arise from astrophysical sources such as subsurface convection (granulation), spots, and stellar oscillations, we routinely monitor the Ca II H and K line emission, or S_{HK} index, in our stars. This index is also a good predictor of the rotational period (Noyes et al. 1984) and the approximate age of F, G, and K main-sequence stars. A comparison of the Ca II H line in HD 3651 is shown relative to the solar spectrum in Figure 1. We measure emission in the Ca II lines and find $S_{\text{HK}} = 0.17$ (on the Mount Wilson scale; Baliunas et al. 1995) for HD 3651, indicating that the star is chromospherically inactive, with a ratio of the H and K flux to the bolometric flux of the star of $\log R'_{\text{HK}} = -5.01$ and an estimated rotational period of $P_{\text{rot}} = 44.5$ days. We expect the total rms jitter from astrophysical noise to be 3–5 m s⁻¹ (Saar, Butler, & Marcy 1998; Saar & Fischer 2000; Santos et al. 2000). Among the 1200 FGKM stars in our sample, we empirically find middle-aged, chromospherically quiet K0 V stars to exhibit rms velocities of 3–5 m s⁻¹.

3. OBSERVATIONS

We have obtained 112 observations of HD 3651 at Lick Observatory over the past 15 years and 26 observations at Keck Observatory over the past 6 years. At both Lick and Keck, we place a special purpose iodine absorption cell in the stellar path to provide wavelength calibration and to model the point-spread function (PSF) of the instrument. The Lick and Keck iodine cells have not been changed during the entire duration of those projects. The temperature of the iodine cell is controlled to $50.0^{\circ}\text{C} \pm 0.1^{\circ}\text{C}$, and the Pyrex iodine cell is sealed so that the column density of iodine remains constant. The iodine absorption lines provide a record of the wavelength scale and the behavior of the spectrometer at the instant of each observation (Butler et al. 1996), preserving the integrity of our contiguous precision

¹ Based on observations obtained at Lick Observatory, which is operated by the University of California, and the W. M. Keck Observatory, which is operated jointly by the University of California and the California Institute of Technology. Keck time has been granted by both NASA and the University of California.

² Department of Astronomy, University of California, Berkeley, CA 94720; fischer@serpens.berkeley.edu.

³ Department of Terrestrial Magnetism, Carnegie Institution of Washington, 5241 Broad Branch Road, NW, Washington, DC 20015-1305.

⁴ UCO/Lick Observatory, University of California, Santa Cruz, CA 95064.

⁵ Center of Excellence in Information Systems, Tennessee State University, 330 10th Avenue North, Nashville, TN 37203; also Senior Research Associate, Department of Physics and Astronomy, Vanderbilt University, Nashville, TN 37235.

⁶ References to published papers and updates on orbital parameters can be found at <http://exoplanets.org>.

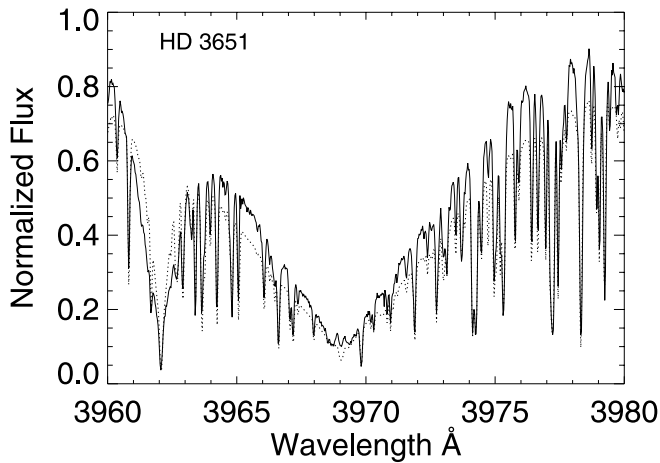


FIG. 1.—Spectrum of HD 3651 near the Ca II H line (solid line) with the National Solar Observatory solar spectrum overplotted (dotted line). The small core emission indicates that this star is chromospherically inactive.

velocity measurements despite drastic changes to the optics of the Lick Hamilton spectrometer and many replacements of the CCD detector. There have not been any significant changes to the Keck High Resolution Echelle Spectrometer (HIRES) system.

The Keck 10 m telescope collects starlight for the HIRES spectrometer (Vogt et al. 1994), which is operated with a resolution of $R \approx 70,000$ and a wavelength range of 3700–6200 Å. At Lick, either the Shane 3 m telescope or the 0.6 m Coudé Auxiliary Telescope (CAT) feed light to the Hamilton echelle spectrometer (Vogt 1987). The Lick Hamilton optics were upgraded in 1994 November by installing a new corrector plate and a new field flattener. Before the upgrade, the PSF was asymmetric, and the resolution of the Hamilton spectrometer was $R \approx 40,000$. Since the upgrade, the PSF is more symmetric, with reduced wings, and the resolution has increased to $R \approx 50,000$. At the same time that the optics were upgraded, a change in the CCD (from 800^2 to 2048^2 pixels) resulted in expanded wavelength coverage. These improvements contributed to a factor of ~ 2.5 higher

Doppler precision. The Doppler shifts of our spectra are determined with the spectral synthesis technique described by Butler et al. (1996).

Individual observations at Lick Observatory (particularly from the CAT) have photon-limited errors with a signal-to-noise ratio of less than 100, so two or three consecutive CAT observations are usually obtained, and the velocities from those consecutive observations are binned. Before the Hamilton optics were upgraded, the mean velocity error for HD 3651 was 8.5 m s^{-1} . Since the upgrade, the mean (binned) velocity error has dropped to 3.4 m s^{-1} . The Lick velocities are plotted in Figure 2a and show peak-to-peak variations of about 50 m s^{-1} , with an rms of 11.4 m s^{-1} . These velocity variations are well above the uncertainty of the individual measurements. A power spectrum of the entire set of Lick velocities is shown in Figure 2b. The strongest peak resides at 62.2 days with a false alarm probability of less than 10^{-4} , based on Monte Carlo simulations in which the velocities are scrambled and power spectra recomputed at the scrambled velocities.

Precise radial velocity observations at Keck are shown in Figure 3a. These velocities carry an average uncertainty of 3.2 m s^{-1} . The rms of the Keck velocities is 8.2 m s^{-1} , with peak-to-peak variations of more than 30 m s^{-1} , again well above the individual measurement errors. The periodogram of the Keck data (Fig. 3b) shows the tallest peak at 20.9 days, nearly one-third the period exhibited in the Lick Observatory velocities. The Keck periodogram also exhibits a marked “hill” of power at 60–63 days, with clear power integrated over that short interval. Such periodogram behavior is consistent with aliasing of the dominant period, accentuated by the sparse sampling of the Keck measurements. The window function can reveal a periodicity of some multiple of the true period, while the true period is suppressed pending more measurements. Keplerian curves with significant eccentricity have natural power at higher frequency because of the Fourier composition of eccentric orbits. In addition, the high eccentricity of the orbit reduces the probability of observing periastron and a velocity minimum in this system, compounding the difficulty in detecting this orbit with less frequent sampling. Thus, the peak at 20

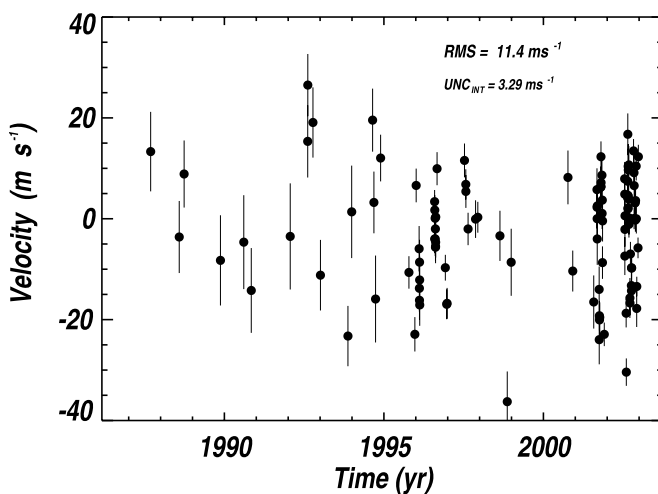


FIG. 2a

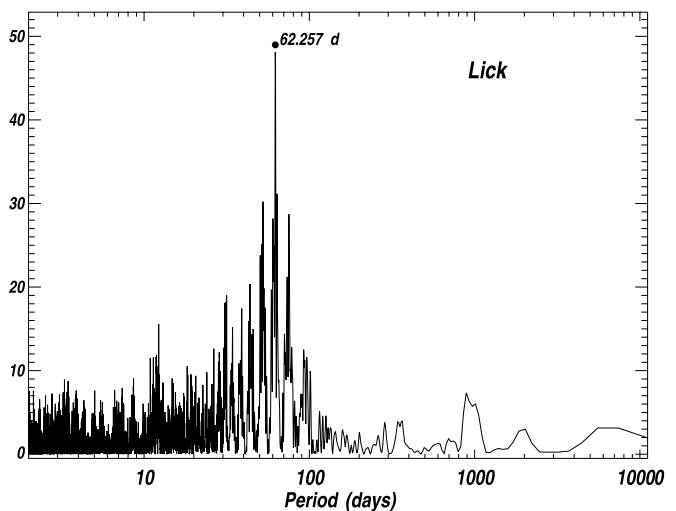


FIG. 2b

FIG. 2.—(a) Lick radial velocities as a function of time for HD 3651. (b) Periodogram of the velocities in (a) showing strong power at 62.2 days.

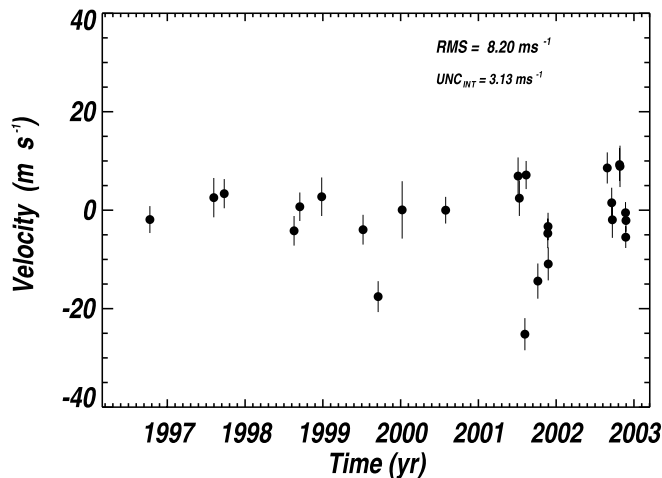


FIG. 3a

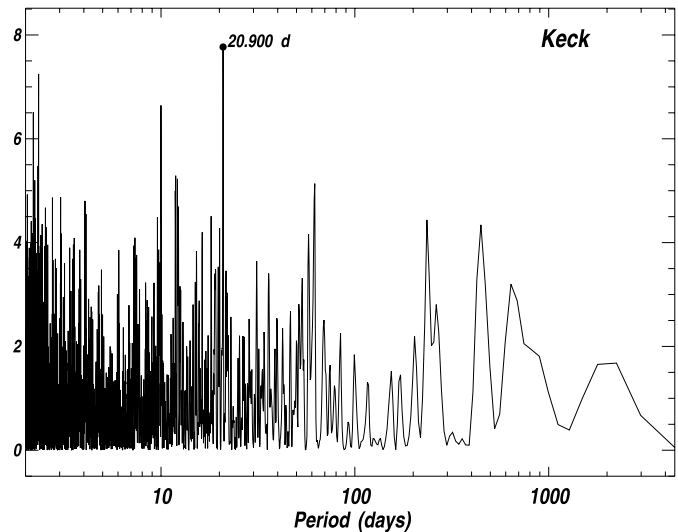


FIG. 3b

FIG. 3.—(a) Keck radial velocities as a function of time for HD 3651. (b) Periodogram of the Keck velocities showing peak power at 20 days, with a weaker peak at 60 days.

days and the mild peak at 60 days in the Keck velocities are consistent with the peak in the Lick velocities at 62 days, but they do not provide strong confirmation of that period.

The Lick and Keck velocities normally have a velocity offset that is best determined by combining the data and minimizing the residuals to the joint Keplerian fit. For HD 3651, this offset is only 1 m s^{-1} . This offset was applied to the Keck velocities, and the combined velocity set is listed in Table 1. The Lick and Keck velocities are phased and plotted in Figure 4a, with the best-fit Keplerian model overplotted as a solid line. The Keplerian model yields an orbital period of $P = 62.23 \pm 0.03$ days, an eccentricity of 0.63 ± 0.03 , and a velocity semi-amplitude of $K = 15.9 \pm 0.6 \text{ m s}^{-1}$. The assumed stellar mass of $0.79 M_{\odot}$ implies a companion mass of $M \sin i = 0.20 M_J$ and a semimajor axis of 0.284 AU. The orbital elements for HD 3651 are listed in Table 2. Although the Keplerian orbit was not independently detected in the

sparser Keck data, when the orbital elements for HD 3651 from the fit to the combined data set are adopted, the fit to the Keck data alone (Fig. 4b) is excellent, with an rms of 3.88 m s^{-1} and $\sqrt{\chi^2} = 1.30$.

We have checked existing high-precision photometric observations of HD 3651 for variability and for a serendipitous transit detection. The T4 0.8 m automatic photoelectric telescope (APT) at Fairborn Observatory⁷ has acquired 403 photometric measurements of HD 3651 during 10 observing seasons from 1994 to 2003. The APT measures the difference in brightness between a program star and nearby comparison stars in the Strömgren *b* and *y* passbands. The observing procedures and data reduction techniques employed with

⁷ Further information about Fairborn Observatory can be found at <http://www.faiobs.org>.

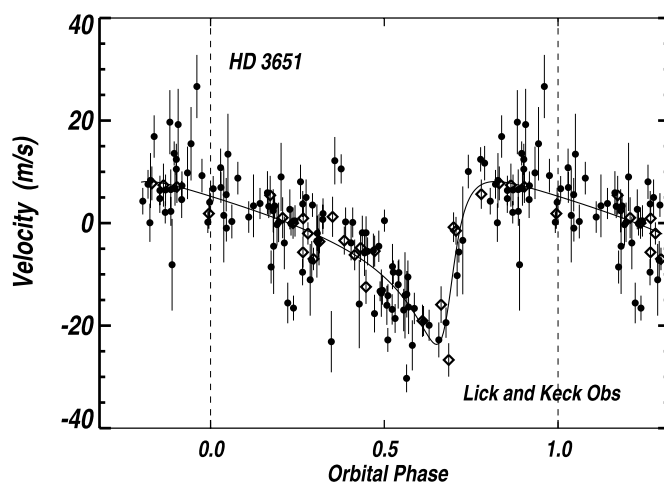


FIG. 4a

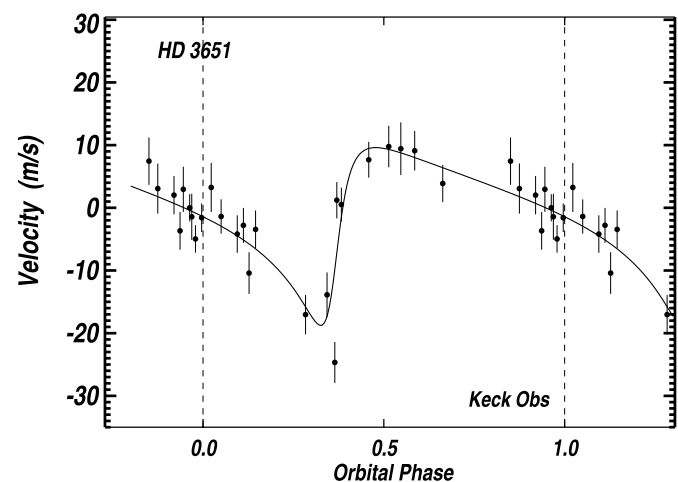


FIG. 4b

FIG. 4.—(a) Combined phased Lick and Keck radial velocities for HD 3651. Lick observations are shown as circles, and the Keck data are plotted as diamonds. The solid line is the radial velocity curve from the best-fit orbital solution, $P = 62.23$ days, $e = 0.63$, and $M \sin i = 0.2 M_J$. The rms to this fit is 6.27 m s^{-1} , with a reduced $\sqrt{\chi^2}$ of 1.83. (b) Plot showing that the Keck data alone support the combined Keplerian fit dominated by the Lick data.

TABLE 1
RADIAL VELOCITIES FOR HD 3651

JD - 2, 440, 000	Radial Velocity (m s ⁻¹)	Uncertainties (m s ⁻¹)	Observatory
7047.854.....	13.74	7.88	Lick
7374.940.....	-3.19	7.15	Lick
7430.758.....	9.30	6.65	Lick
7846.849.....	-7.82	8.95	Lick
8113.959.....	-4.21	9.31	Lick
8199.717.....	-13.79	8.41	Lick
8645.680.....	-3.08	10.52	Lick
8845.939.....	15.77	7.16	Lick
8846.983.....	26.93	6.16	Lick
8905.861.....	19.52	6.97	Lick
8991.737.....	-10.76	7.00	Lick
9306.678.....	-22.83	5.98	Lick
9349.646.....	1.80	9.17	Lick
9588.915.....	19.98	6.25	Lick
9603.889.....	3.66	6.12	Lick
9622.835.....	-15.49	8.62	Lick
9680.681.....	12.47	4.63	Lick
10004.929.....	-10.21	3.22	Lick
10072.696.....	-22.48	3.41	Lick
10087.678.....	7.03	3.34	Lick
10121.626.....	-5.52	4.50	Lick
10124.631.....	-13.36	4.62	Lick
10125.623.....	-15.74	3.82	Lick
10126.629.....	-8.18	4.42	Lick
10127.652.....	-11.71	4.66	Lick
10128.633.....	-16.66	4.14	Lick
10298.990.....	3.82	2.31	Lick
10300.006.....	-3.58	2.81	Lick
10300.881.....	2.15	2.97	Lick
10304.920.....	0.53	2.82	Lick
10305.910.....	-3.56	3.41	Lick
10307.921.....	-1.58	3.32	Lick
10308.860.....	-5.22	2.73	Lick
10309.904.....	-5.07	3.32	Lick
10310.872.....	-4.23	3.06	Lick
10311.884.....	0.77	2.16	Lick
10326.907.....	10.35	3.28	Lick
10366.925.....	-3.11	2.74	Keck
10421.677.....	-9.28	2.56	Lick
10437.723.....	-16.54	2.96	Lick
10441.698.....	-16.34	3.06	Lick
10640.977.....	11.99	3.35	Lick
10655.974.....	7.24	2.99	Lick
10656.929.....	5.84	3.26	Lick
10667.033.....	1.34	3.99	Keck
10681.973.....	-1.60	3.21	Lick
10716.051.....	2.15	2.97	Keck
10767.720.....	0.36	3.73	Lick
10793.708.....	0.72	3.06	Lick
11044.061.....	-5.39	3.01	Keck
11046.934.....	-2.96	4.98	Lick
11071.029.....	-0.51	2.89	Keck
11130.693.....	-35.84	5.99	Lick
11173.824.....	1.53	3.92	Keck
11175.627.....	-8.20	6.65	Lick
11368.050.....	-5.17	3.03	Keck
11438.846.....	-18.76	3.14	Keck
11551.688.....	-1.15	5.83	Keck
11756.006.....	-1.21	2.71	Keck
11825.747.....	8.62	5.33	Lick
11880.668.....	-9.94	4.06	Lick
12096.111.....	5.72	3.79	Keck
12102.020.....	1.23	3.60	Keck
12120.894.....	-16.08	5.27	Lick

TABLE 1—Continued

JD - 2, 440, 000	Radial Velocity (m s ⁻¹)	Uncertainties (m s ⁻¹)	Observatory
12128.082.....	-26.39	3.26	Keck
12133.920.....	5.94	2.86	Keck
12157.848.....	6.20	4.22	Lick
12158.878.....	2.71	4.19	Lick
12159.844.....	0.44	3.85	Lick
12160.875.....	-3.58	5.13	Lick
12161.856.....	2.98	3.90	Lick
12182.806.....	-13.58	4.54	Lick
12183.795.....	-23.55	4.89	Lick
12185.801.....	-18.80	2.93	Lick
12186.800.....	-19.63	3.03	Lick
12188.947.....	-15.61	3.58	Keck
12189.829.....	-19.12	2.96	Lick
12200.822.....	6.67	2.87	Lick
12201.829.....	6.77	3.00	Lick
12202.762.....	6.83	3.94	Lick
12203.760.....	12.73	3.05	Lick
12204.767.....	7.59	2.78	Lick
12214.775.....	9.07	3.18	Lick
12216.728.....	1.48	3.08	Lick
12218.747.....	4.12	3.04	Lick
12220.735.....	-8.27	3.22	Lick
12221.793.....	0.00	4.09	Lick
12235.698.....	-5.91	2.99	Keck
12236.759.....	-4.52	2.78	Keck
12237.729.....	-12.13	3.33	Keck
12241.639.....	-22.49	2.33	Lick
12474.923.....	8.35	3.34	Lick
12475.924.....	5.29	3.52	Lick
12476.936.....	-6.97	3.76	Lick
12477.935.....	-1.69	3.43	Lick
12478.914.....	1.02	2.87	Lick
12491.866.....	-18.31	2.82	Lick
12493.918.....	-29.99	2.72	Lick
12508.908.....	4.57	2.59	Lick
12509.844.....	7.87	2.80	Lick
12510.944.....	17.18	4.13	Lick
12511.961.....	5.08	2.79	Lick
12512.932.....	2.39	2.16	Lick
12513.934.....	2.58	2.82	Lick
12514.915.....	10.82	3.46	Lick
12515.020.....	7.38	3.16	Keck
12515.869.....	4.88	3.60	Lick
12516.917.....	10.10	5.12	Lick
12520.885.....	4.36	2.82	Lick
12522.843.....	11.10	3.73	Lick
12523.877.....	-0.69	2.61	Lick
12524.856.....	0.61	3.30	Lick
12534.869.....	-15.28	3.96	Lick
12535.819.....	0.30	3.06	Keck
12535.897.....	-16.28	2.43	Lick
12551.823.....	-12.82	2.81	Keck
12552.811.....	-13.87	2.24	Lick
12553.773.....	-9.29	2.30	Lick
12554.767.....	-9.36	2.56	Lick
12572.760.....	8.05	3.30	Lick
12574.835.....	7.70	4.20	Lick
12576.761.....	13.88	2.35	Keck
12581.737.....	9.56	3.28	Keck
12582.787.....	0.48	2.12	Lick
12583.747.....	7.00	2.48	Lick
12593.699.....	3.56	2.29	Lick
12594.747.....	3.65	2.51	Lick
12597.685.....	0.16	2.29	Lick
12599.782.....	4.03	2.54	Lick

TABLE 1—Continued

JD - 2,440,000	Radial Velocity (m s ⁻¹)	Uncertainties (m s ⁻¹)	Observatory
12600.717.....	-1.72	2.17	Lick
12601.712.....	-6.69	2.19	Lick
12602.777.....	-3.30	2.28	Keck
12606.667.....	10.87	2.85	Keck
12608.735.....	0.43	2.92	Keck
12612.637.....	-17.36	3.67	Lick
12613.635.....	-13.00	1.93	Lick
12627.747.....	-5.35	2.05	Lick
12631.640.....	12.73	2.37	Lick

NOTE.—Table 1 is also available in machine-readable form in the electronic edition of the *Astrophysical Journal*.

this APT are described in Henry (1999). The external precision of the photometric observations, defined as the standard deviation of a seasonal set of differential magnitudes, is typically around 0.0014 mag for the T4 APT, as determined from pairs of constant stars.

The differential magnitudes of HD 3651 minus the comparison star HD 3690 (= HR 167 = 55 Psc; $V = 5.36$, $B - V = 1.160$, K0 Iab) in the combined Strömgren $(b + y)/2$ passband are plotted in the top panel of Figure 5. The APT acquired an average of 40 measurements in each of the 10 observing seasons. The standard deviations of a single observation from the seasonal means ranged from 0.0012 to 0.0018 mag in the 10 seasons, with a mean of 0.0015 mag, so the night-to-night scatter in the observations is essentially equal to the typical measurement uncertainty. The 10 seasonal means have a range of 0.0016 mag and a standard deviation of 0.0005 mag, compared to our typical measurement precision of 0.0002 mag for seasonal means. Thus, HD 3651 and/or its comparison star probably vary slightly from year to year. Given the spectral type of the comparison star, we suspect it as the most likely source of the variability.

Before further analysis, we removed the long-term variability in the data set by offsetting seasons 2–10 so that their seasonal means matched that of the first season. Periodogram analysis of the resulting data set showed no hint of periodicity between 1 and 100 days, as expected from the very low scatter in the observations. In particular, we find no rotation signal in the vicinity of the estimated 44.5 day rotation period, so we are not able to measure the star’s

TABLE 2
ORBITAL PARAMETERS FOR HD 3651

Parameter	Value
P (days).....	62.23 (0.03)
T_p (JD).....	2,452,501.7 (1.2)
e	0.63 (0.04)
ω (deg).....	235.7 (6.6)
K_1 (m s ⁻¹).....	15.9 (1.7)
$a_1 \sin i$ (AU).....	7.3E-05
f_1 (m) (M_\odot).....	1.346E-11
a_{rel} (AU).....	0.284
$M \sin i$ (M_J).....	0.20
N_{obs}	138
rms (m s ⁻¹).....	6.27
Reduced $\sqrt{\chi^2}$	1.83

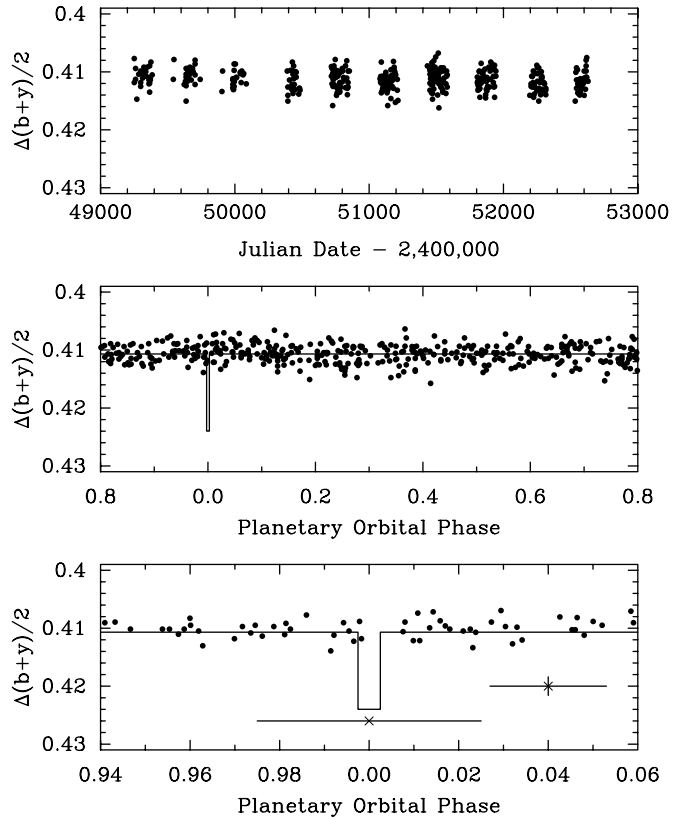


FIG. 5.—Photometric observations of HD 3651 acquired with the T4 0.8 m APT at Fairborn Observatory. The star is constant to better than 0.001 mag on both short and long timescales (top), with no evidence for any periodicity. There is no photometric variability on the radial velocity period to a limit of 0.0002 mag (middle), supporting the planetary interpretation of the radial velocity variations. There is no evidence for photometric transits (bottom), and they are ruled out to a confidence level of 87%.

rotation period directly since it has such low surface magnetic activity. With the orbital elements in Table 2, we computed a time of conjunction with the planet in front of the star (i.e., a predicted time of transit) to be JD 2,452,487.6, with an uncertainty of roughly 1.6 days. The observations were phased with this time of conjunction and the 62.23 day planetary orbital period and are plotted in the middle panel of Figure 5. The semiamplitude of a least-squares sine fit to the phased data is 0.0002 ± 0.0001 mag. The 0.03 day uncertainty in the period, combined with the 10 year range in the data set, produces relative phase uncertainties across the data set of up to ± 0.013 phase units. Even though this is relatively small and probably insignificant for the sine-curve fit, we repeated the least-squares analysis with multiple trial periods within the range of uncertainty, with no significant difference in the resulting semiamplitude. Thus, our extremely low limit to any intrinsic stellar brightness changes on the planetary orbital period provides strong support for the planetary interpretation of the radial velocity variations. The star’s low activity level ($\log R'_{\text{HK}} = -5.01$), the very low limit of photometric variability on the radial velocity period, and the strong coherence of the radial velocity variations over the 15 year span of the velocity observations make it very unlikely that intrinsic stellar activity is the cause of the velocity variations.

The photometric observations around the phase of predicted transit are replotted in the lower panel of Figure 5, with an expanded scale on the abscissa. The predicted depth

and duration of the transit are shown schematically, assuming a planetary radius of $1.0R_J$ and a stellar radius of $0.93R_\odot$ estimated from the *Hipparcos* parallax and photometry. The eccentric planetary orbit is orientated with respect to our line of sight such that we get no advantage from the close periastron approach in increasing the transit probability; conjunction occurs with a star-planet separation comparable to the orbital semimajor axis. The error bar under the transit window shows the estimated uncertainty in the time of transit, while the error bar in the lower right shows the uncertainty in the magnitude and phase of a single observation. Given the uncertainty in the period (and the resulting phase smearing) along with the uncertainty in the time of conjunction, we cannot completely eliminate the possibility of transits in this system. For example, if the period is precisely our quoted 62.23 days and the true time of conjunction is about 0.003 phase units later than predicted, then we would have no observations in the transit window. However, with 403 observations taken at random with respect to the planetary period and the predicted transit duration of 0.005 phase units, we would expect two of our observations to fall in any transit window. The probability of at least one of our observations landing in a transit window of 0.005 phase duration is 87%. Thus, in spite of the uncertainties in the planetary orbital period and the time of conjunction, we can still rule out transits to this high level of confidence.

4. DISCUSSION

Observations at Lick and Keck Observatories have revealed a sub-Saturn mass planet orbiting HD 3651, a K0 V star. The Keplerian orbit has a period of 62.23 days and an orbital eccentricity of 0.63. With an assumed stellar mass of $0.79M_\odot$, the inferred $M \sin i$ is $0.20M_J$, with a semimajor axis of 0.284 AU. As determined from high-resolution spectra of the Ca II H and K lines and precise photometry, HD 3651 is both chromospherically inactive and photometrically stable. In particular, HD 3651 has been photometrically stable within measurement errors (0.001 mag) over 10 seasons. There is no photometric variability near the Doppler-derived orbital period and no evidence for a serendipitous photometric transit.

HD 3651 has been on our Lick planet search survey since 1988 and on the Keck survey for 6 years. The rms velocity scatter was under 12 m s^{-1} in the Lick radial velocity data and less than 8 m s^{-1} in the Keck data. Although low, this rms scatter exceeds the internal errors by a factor of 2 or 3. In principle, this was a signal that might have been detected sooner, yet it slipped through our “detection net.” There were a few factors that conspired to hide this planet. First, the rms scatter is small enough that astrophysical sources or systematic errors were a concern. Second, because of the high orbital eccentricity in this system, the periastron velocity departures were rare. For most of the orbit, the velocities showed less than 2σ rms scatter. Finally, the periodogram analysis of our velocities did not show a strong power peak until recently. The breakthrough in this case was that we began observing HD 3651 more frequently during the last 2 years, largely to understand systematic errors at Lick and the occasional velocity departures seen in HD 3651. After acquiring a higher observing cadence, the phase coverage for the 62 day Keplerian orbit was improved, and the periodogram analysis of our Lick velocities showed strong power. The Keplerian orbit that we then derived phased up

over the long time baseline of Lick observations and with the 6 years of Keck velocities.

At a distance of just 11 pc, this chromospherically quiet K0 V star is a prime target for the *Space Interferometry Mission* and other NASA planet search missions. Knowledge regarding the existence of this companion will bear upon decisions such as (1) the selection of this star for particular missions, (2) the probability of detecting terrestrial planets in the star’s habitable zone, (3) the interpretation of mission data, and (4) the timing and frequency of mission observations.

The original Lick survey (predating 1997) is an excellent sample for addressing the statistics of extrasolar planets. This sample of stars originally numbered 100, but only 51 of those stars are high Doppler precision stars where planets can be detected. Some of the original Lick stars turned out to be spectroscopic binaries, some were chromospherically active or rapidly rotating, a few were evolved stars, and all of the faint M dwarfs were transferred to the Keck project, where the improved signal-to-noise ratio yields higher velocity precision.

Among that sample of 51 Lick target stars, we have detected two triple-planet systems (*v* And and 55 Cnc), one double-planet system (47 UMa), and five single-planet systems (70 Vir, τ Boo, ϵ Eri, 16 Cyg B, and HD 3651). Other stars with planets in the original Lick sample (51 Peg, ρ CrB, and Gl 876) have been excluded from this count: 51 Peg was added after detection by Mayor & Queloz (1995), ρ CrB was added to follow up on an Advanced Fiber Optic Echelle spectrometer detection (Noyes et al. 1997), and Gl 876 is an M dwarf (Marcy et al. 2001) that has been transferred to Keck. Thus, from the sample of 51 stars, the current fraction of extrasolar planetary systems is 8/51, or 15%.

However, the fraction of detected planets in this sample will certainly grow. We have just begun to scrutinize these stars with higher precision and cadence for lower amplitude signals. Like HD 3651, there are other stars with low-amplitude rms velocity scatter where sub-Saturn mass planets may yet be detected.

We thank David Mitchell, Bernie Walp, Eric Nielsen, Jason Wright, John Johnson, and Julia Kregenow for taking spectra of HD 3651 at Lick Observatory. We gratefully acknowledge the dedication of the Lick Observatory staff, particularly Tony Misch, Keith Baker, Kostas Chloros, Wayne Earthman, John Morey, and Andy Tullis. We thank Richard Stover and his lab for ongoing support with hardware and CCD detectors at Lick. We appreciate support by NASA grant NAG5-75005, NSF grant AST 99-88358 (to S. S. V.), NSF grant AST 99-88087, and NASA grant NAG5-12182 and travel support from the Carnegie Institution of Washington (to R. P. B.). G. W. H. acknowledges support from NASA grants NCC5-96 and NCC5-511 as well as NSF grant HRD 97-06268. We are also grateful for support by Sun Microsystems. We thank the NASA and UC telescope assignment committees for allocations of telescope time, especially Robert Kraft and Joseph Miller for their foresightful allocations of Lick Observatory telescope time. This research has made use of the SIMBAD database operated at CDS, Strasbourg, France. The authors wish to extend special thanks to those of Hawaiian ancestry on whose sacred mountain of Mauna Kea we are privileged to be guests. Without their generous hospitality, the Keck observations presented herein would not have been possible.

REFERENCES

- Baliunas, S. L., et al. 1995, *ApJ*, 438, 269
Butler, R. P., Marcy, G. W., Vogt, S. S., Fischer, D. A., Henry, G. W., Laughlin, G. P., & Wright, J. T. 2003, *ApJ*, 582, 455
Butler, R. P., Marcy, G. W., Williams, E., McCarthy, C., Dosanji, P., & Vogt, S. S. 1996, *PASP*, 108, 500
Butler, R. P., et al. 2002, *ApJ*, 578, 565
Drilling, J. S., & Landolt, A. U. 2000, in *Allen's Astrophysical Quantities*, ed A. N. Cox (4th ed.; New York: Springer), 389
ESA. 1997, *The Hipparcos and Tycho Catalogs* (ESA-SP 1200; Noordwijk: ESA)
Henry, G. W. 1999, *PASP*, 111, 845
Marcy, G. W., Butler, R. P., Fischer, D. A., Vogt, S. S., Lissauer, J. J., & Rivera, E. J. 2001, *ApJ*, 556, 296
Marcy, G. W., Butler, R. P., & Vogt, S. S. 2000, *ApJ*, 536, L43
Mayor, M., & Queloz, D. 1995, *Nature*, 378, 355
Noyes, R. W., Hartmann, L., Baliunas, S. L., Duncan, D. K., & Vaughan, A. H. 1984, *ApJ*, 279, 763
Noyes, R. W., Jha, S., Korzennik, S. G., Krockenberger, M., Nisenson, P., Brown, T. M., Kennesly, E. J., & Horner, S. D. 1997, *ApJ*, 483, L111
Pepe, F., Mayor, M., Galland, F., Naef, D., Queloz, D., Santos, N. C., Udry, S., & Burnet, M. 2002, *A&A*, 388, 632
Saar, S. H., Butler, R. P., & Marcy, G. M. 1998, *ApJ*, 498, L153
Saar, S. H., & Fischer, D. A. 2000, *ApJ*, 534, L105
Santos, N. C., Mayor, M., Naef, D., Pepe, F., Queloz, D., Udry, S., & Blecha, A. 2000, *A&A*, 361, 265
Tinney, C. C., Butler, R. P., Marcy, G. W., Jones, H. R. A., Penny, A. J., McCarthy, C., Carter, B., & Bond, J. 2003, *ApJ*, submitted
Vogt, S. S. 1987, *PASP*, 99, 1214
Vogt, S. S., et al. 1994, *Proc. SPIE*, 2198, 362